# The effect of mesoporous silica impregnation on tribo-electrification characteristics of flurbiprofen

Mohammad S. Afzal [a], Faiza Zanin [a], Muhammad Usman Ghori [b], Marta Granollers [c], Enes Šupuk [a] *

[a] Department of Chemical Sciences, School of Applied Sciences, University of Huddersfield, Huddersfield HD1 3DH, UK
[b] Department of Pharmacy, School of Applied Sciences, University of Huddersfield, Huddersfield HD1 3DH, UK
[c] European Bioenergy Research Institute, Aston University, Birmingham B4 7ET, UK

*corresponding author ( E.Supuk@hud.ac.uk )

## Graphical abstract;

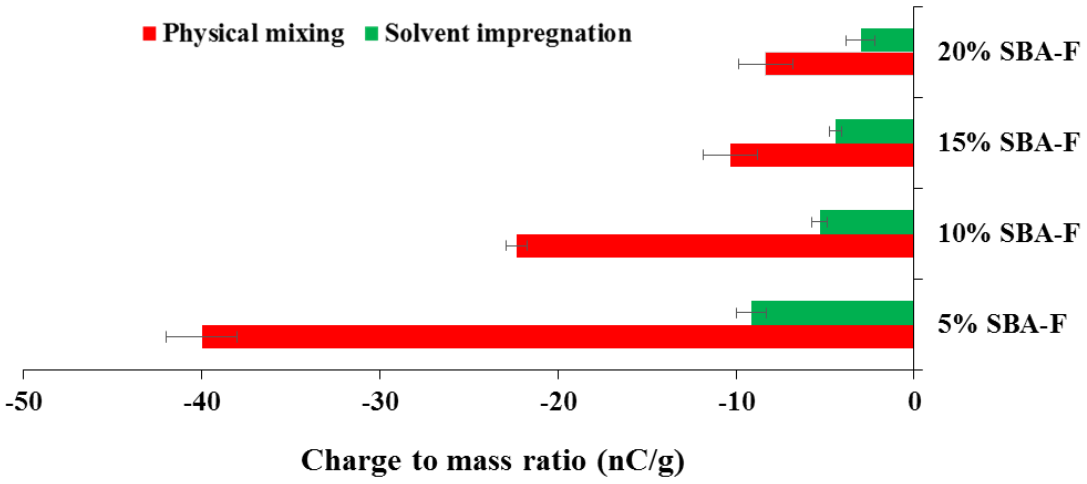

## Abstract

Tribo-electrification is a common occurrence within the pharmaceutical industry where solid dosage forms constitute majority of pharmaceutical formulations. Tribo-electrification of powders leads to a range of complications such as adhesion of particulate material to the processing equipment resulting in segregation, affecting the content uniformity. Flurbiprofen, a highly charging material, was used as a model drug to investigate the tribo-electrification and adhesion characteristics by impregnating the model drug inside a mesoporous silica matrix. The model drug was impregnated using i) solvent loading, and ii) physical mixing methods, at varying degree of silica to drug ratio (5-20 % w/w). The resulting mixtures were tribo-charged using a custom built device based on a shaking concept inside a stainless steel capsule, consisting of a Faraday cup and connected to electrometer. The electrostatic charge and the percentage adhesion of Flurbiprofen were reduced in both drug loading methods. The solvent impregnation method using acetone was more successful at reducing the electrostatic charge build up on flurbiprofen than physical powder mixing. The percentage adhesion to the shaking capsule was reduced notably as a result of loading the drug in the SBA-15 porous network. The results illustrate that the incorporation of highly charged model drug inside a low-charging pharmaceutical carrier system to be an effective approach in control the induction of tribo-electrification phenomena during powder processing.



## Keywords

Mesoporous Silica, SBA-15, Tribo-electrification, Flurbiprofen, Drug loading, Electrostatics,

# 1- Introduction

In many industrial applications such as pharmaceutical, detergent, cosmetics and food manufacturing, powder handling is a challenging process due to complications arising during the manufacturing process. A common obstacle faced in powder handling is the powder tribo-electrification phenomenon (Watanabe et al., 2007; Kaialy 2016). The phenomenon is complex and not well understood due to many factors affecting the charge transfer process. Currently, three fundamental mechanisms contributing to charge generation by tribo-electrification are most commonly reported include material transfer, ion transfer and electron transfer. The most widely accepted theory is electron transfer, working on a principle of varying work function (Ø) of material, Ø is the minimum energy required to remove electrons in the outer electron shell of an atom. Resulting in the flow of electron from the lower work function towards the higher, inducing a potential difference across the particle surface, allowing for charge to transfer (Cross, 1987).

Tribo-electrification occurs when particles come into contact with one another or the walls of processing equipment in unit operations such as mixing, conveying, granulating or blending when these two dissimilar materials make contact by impaction or shearing and are subsequently separated, holding any charge transferred (Matsusaka et al., 2010). Charged materials have a tendency to adhere or repel powder particles, resulting in flowability issues and potentially may lead to blockages of pipes by particle adhesion to the walls of processing equipment (Matsusaka and Masuda, 2003). Within the pharmaceutical industry this can be problematic and in extreme cases, tribo-electrification of material may lead to dust explosions (Šupuk et al., 2011). These challenges are faced during common powder handling processes such as milling, filling and compaction, in addition to a rise is unit operation problems leading to segregation of materials, impacting the quality of the end product by jeopardising the content

uniformity of the batch (Lakhani and Deshpande, 2013). Investigating alternative methods for charge control is therefore crucial.

SBA-15 is a highly porous material with a rising interest for its application in drug delivery (Colilla et al., 2015; Yu and Zhai, 2009). It is comprised of nano-sized cylinder filled with regular arranged pores, expected to provide a more versatile drug delivery material (Song et al., 2005). In this paper the principle of the highly charging material is embedded within the silica pores, to provide a low-charging carrier system. The model drug was impregnated using i) solvent loading, and ii) physical mixing methods, at different silica ratios and the drug loading ability was compared. The purpose of drug loading would allow for the API to be administered in its original form, without the need for lengthy steps to aid in material handling properties whilst maintaining physicochemical properties (Ghori, 2014; Ghori et al., 2015). Currently no work has been reported on the effects of SBA-15 upon the charging tendency of a pharmaceutical material, prompting the purpose of this study.

As many active pharmaceutical ingredients (APIs) have a propensity to become electrostatically charged, various techniques are utilised to aid material handling by improving the physicochemical properties, however, these can lead to further complications (Šupuk et al., 2013) such as extra steps  increasing processing times. For the purpose of this study, FBP) was chosen as the model material due to its crystalline nature and poor adhesion properties, factors which are characteristic of materials possessing a high propensity for tribo-charging (Šupuk et al., 2013). Murtomaa et al believe that the amorphicity has a measurable effect on the tribo-charging of powders (Murtomaa et al., 2002) A study undertaken by Carter et al investigates the tribo-electrification of spray dried and crystalline lactose which concluded significant differences in charge values between the two lactose powders under the same conditions (Carter et al., 1998). A more recent studies have examined the tribo-electrification of

amorphous salbutamol sulfate which was more electropositive than jet-milled crystalline particles (Kwok and Chan, 2008). Such results could have been seen due to different surface energies between crystalline and amorphous materials leading to varying charge values (Zhang et al., 2006). FBP is well known for its poor compaction, solubility and dissolution (Ghori et al., 2014a; Rudrangi et al., 2016) properties due to its propensity to adhere to the punch surfaces, FBP has been reported as a highly sticking compound (Paul et al., 2017). The adhesion properties may be due to the ability of the powder to withhold high levels of electrostatic charge, reducing the propensity for gaining charge may lead to an improvement in material handling as well as compaction properties (Šupuk et al., 2013). In this study we have incorporated FBP within the extremely porous SBA-15 material, which possesses a large surface area, allowing for the pores to be filled with the drug, with an aim reduce the charge propensity whilst maintaining therapeutic potency, as well as quantifying the percentage adhesion of drug material to the shaker walls. The model would then be used to explore other systems to investigate their charging tendency as a result of being loaded within the low-charging carrier system.

# 2- Materials and Methods

## 2.1- Materials

Flurbiprofen was purchased from Aesica Pharmaceutical Ltd. (Cramlington, UK) and Mesoporous silica (SBA-15) was obtained from ACS Material (California, USA). The solvent used was Acetone, purchased from Fisher Scientific (Loughborough, UK).

## 2.2- Methods

### 2.2.1- Fractionation of SBA-15 and FBP particle size

Particle size fractions of SBA-15 (150–250 μm) and Flurbiprofen (38–63 μm) were obtained through mechanical sieving. All the powders were stored at ambient temperature (18–24 °C) and humidity (RH 36%–44%) before any further investigations.

### 2.2.1- Development of SBA-15: FBP powder mixtures

The binary mixtures of SBA-15 and FBP of varying SBA-15 to FBP ratios (5-20 %w/w) were prepared using two loading methods; solvent impregnation and powder impregnation, allowing for a comparison of drug distribution throughout the mesoporous silica matrix.

#### 2.2.1.1- Solvent impregnation method

SBA-15: FBP mixtures were prepared by dissolving 1.5g of pure drug in 5 ml of acetone. After the drug has completely dissolved, the ratio dependant quantity of SBA-15 was added, and the solution was stirred for 5 min. The samples were initially dried at room temperature for 24 h followed by a further 24 h drying at 40 °C using conventional oven.

#### 2.2.1.2- Powder physical mixing

SBA-15: FBP physical mixtures were prepared by placing 5g of drug and the relevant ratio of SBA-15 in a glass container and mixed for 10 minutes at 49 rpm using a Turbula mixer (Glen Creston Ltd, UK). The container was left for 2 days for any potential charge to dissipate.

## 2.2.2- Physicochemical characterisation of powder mixtures

#### 2.2.2.1- Differential Scanning Calorimetry (DSC) studies

Differential Scanning Calorimetry (DSC) was undertaken using Mettler Toledo SC 821, Mettler-Toledo Ltd., Leicester, UK. Specimens of 5-10 mg were placed in vented aluminium pans under nitrogen purge at 50 ml $min^{-1}$, over a range of 25-300°C at a heating rate of 10°C $min^{-1}$. An estimated percent crystallinity of the binary mixtures was assessed using Eq. 1, relative to the melting enthalpy of crystalline FBP as a reference.

$$\%\ Relative\ crystallinity = \left(\frac{melting\ enthalpy\ of\ the\ sample}{melting\ enthalpy\ of\ the\ reference\ standard}\right) X\ 100 \qquad \text{Eq. 1}$$

#### 2.2.2.2- Thermogravimetric analysis (TGA)

Thermogravimetric analysis (TGA) was performed using a Mettler Toledo TGA, Mettler-Toledo Ltd., Leicester, UK, samples between 5-10 mg and a temperature range of 25-500°C at a heating rate of 5°C $min^{-1}$ were used. The process was carried out under a nitrogen purge at a constant flow rate of 50 ml $min^{-1}$.

#### 2.2.2.3- Powder X-Ray diffraction (XRD)

The Bruker $D_2$ Phaser XRD diffractometer by Bruker, Coverntry, UK was used to obtain patterns for the parent drug (FBP) and SBA-15 as well as the powder mixes. The sample powders were scanned at a $2\theta$ (5° -100°) at a scanning rate of 1.5 $min^{-1}$.

#### 2.2.2.4- Content uniformity analysis

The concentration of FBP was quantified by UV-Vis spectrophotometry, (Jenway 6305 UV-Vis Spectrophotometer, λ max = 247 nm) (Verma et al., 2016) where 10 mg of sample was randomly obtained from each batch (n=3), dissolved in 100 ml of phosphate buffer at pH 7.2 for 24 hours (Ghori et al., 2014b). The sample was then filtered using a 0.45ml PTFE syringe filter. The acceptance limit was in the 95-105 % range (BP 2012).

#### 2.2.3.5- Brunauer–Emmett–Teller (BET) analysis

Pore size and surface area was analysed using the Micromeritics 2020 apparatus. The study was carried out at 77 K, prior to analysis the samples were de-gassed in a vacuum oven at 100 °C for 10 hours, using a FlowPrep 060. The surface area of the sample was calculated using Brunauer–Emmett–Teller (BET) equation from the adsorption data (Brunauer et al., 1938). The pore-size distribution results are generated from the adsorption branches of the nitrogen isotherms using the BJH model (Barrett et al., 1951). Each sample was analysed in duplicate.

### 2.2.3- Tribo-electrification studies

The charge to mass ratio (*Q/M*) of the materials was obtained using a shaking concept originally described by (Šupuk et al., 2009) and adopted in various studies (Asare-Addo et al., 2013; Ghori et al., 2014; Ghori 2014; Ghori et al., 2015 ). Briefly, Powder (~0.1 g) was placed inside a stainless steel cylindrical container (10 mL) and shaken in a horizontal direction (Retsch MM 400) for 0.5, 2, 5 and 10 min at a vibration frequency of 20 Hz. The charged powder particles were then poured into a Faraday cup, connected to an electrometer (Keithley Model 6514). A Faraday cup comprises two concentric cups made up of a conducting material. The outer cup is slightly larger and acts as an electrical shield and a lid covers it. Both are very important to prevent the effect of any extraneous electric fields. The inner cup is directly attached to an

electrometer for charge measurement and can be removed to measure the weight of the sample poured. The two cups are separated by a PTFE insulator. As charged samples are loaded into the inner Faraday cup, this induces an equal but opposite charge on the wall of inner faraday cup, providing the net charge on the object. The resolution of the charge measurement was in nano-Coulombs (nC). The charge to mass ratio (Q/M) was calculated by dividing the final charge with the final mass of the respective powder. Each tribo-electric charging test was repeated three times and the shaking container was cleaned between each test by washing with isopropyl alcohol, rinsing with water and drying with compressed air to remove any residual deposits, impurities and surface charges. All the powder samples were stored overnight at an ambient temperature (21–23.1 °C) and humidity (RH 36%–48%) for dissipation of tribo-charging. Studies were carried out at an ambient temperature (18–24 °C) and humidity (RH 36%–44%). Maximum charge was gained after 5 min shaking for FBP and SBA-FBP powder mixtures. Maximum charge acquisition data ($Q_{max}$) are presented as charge to mass ratio (Q/M) at the end of each tribo-electrification experiment (n = 3).

### 2.2.4- Powder surface adhesion studies

Powder particle adherence to the surface of the stainless steel container used in the tribo-electrification studies was calculated from mass difference by deducting the final amount recovered (post-shaking and tapping) from the initial amount of sample loaded into the shaking vessel and powder mass loss was demonstrated as a percentage (%) of powder adhesion (Ghori 2014; Ghori et al., 2014; Ghori et al., 2015).

## 3- Results and discussion

### 3.1- Thermal Analysis

Thermal analysis was carried out using DSC and TGA. In the DSC traces obtained for SBA-15, the melting peak was not observed in the (Figure 1) temperature range tested (25 – 350 °C) due to its high melting point of >1600 °C. Table 1 illustrates the melting point and % relative crystallinity for all samples for both methods. The melting point corresponding to the parent drug is a sharp endothermic melting peak at ~116°C. However, melting endotherms for the binary mixtures showed reduced intensity as the percentage of SBA increased for both loading methods, this may be due to the crystalline material entering the pore matrix of the SBA-15, so a reduced amount of material is available, also SBA-15 did not present a melting enthalpy within the chosen temperature range, resulting in a reduction in intensity of the melting endotherm formed by the binary powder mixtures. From the DSC (Figure 1 and Table 1), data it is evident that the introduction of SBA-15 has no chemical influence upon FBP as such changes would influence the tribo-electrification results, strongly indicating that the suppression of charge propensity is due to the drug loading within the pore network of the mesoporous silica. The enthalpy of FBP was 116.5 $J/g^{-1}$ in contrast to 20% SBA by physical mixing at 71.5 $J/g^{-1}$, signifying a decrease in crystallinity as a result of loading the FBP within the pores of the SBA-15. The results show approximately 40-50% reduction in crystallinity at the highest silica loading concentration in contrast to the pure drug material, with solvent impregnation showing a greater reduction in crystallinity for all SBA-15: FBP mixtures.

Thermogravimetric analysis was undertaken in order to determine successful uptake of FBP onto SBA-15 and results are depicted in Figure 2. The total weight loss of 97.5% was observed for FBP (Figure 2) at 270°C. The drug loading fraction can be estimated from the ratio of the weight loss occurring between 100 and 500°C from the initial weight, considering the limitation of distinguishing any drug sample on the surface of SBA-15 from drug material loaded within the pores. For samples prepared by both methods, the weight loss remained constant initially and the loss initiated at approximately 175-200°C, beyond this point the mass

decreased rather significantly; reaching a state of maximum degradation, in the case of FBP the weight loss was ~97% in comparison the drug loaded within SBA-15, as little as 5% of the silica showed a ~65% reduction in weight for solvent impregnation and ~55% for the physical mixture, indicating successful drug loading of the drug material within the pores rather than coating the surface of the mesoporous silica . As the SBA percentage increase the percentage weight loss decreased, where 20% SBA-15 showed a reduction by ~65% in comparison to FBP at 97% (Figure 2). Both loading methods presented a similar pattern to the pure FBP. TGA analysis showed no weight loss that would be indicative of hydrate/solvate formation, which may have occurred during the solvent impregnation method, the formation of a hydrate/solvate may influence tribo-electrification of a material.

## 3.2- Powder X-ray diffraction

XRD was used to confirm sample crystallinity for the FBP, SBA-15, and the binary mixtures of FBP and SBA-15 prepared by solvent impregnation as well as physical impregnation. The crystallinity is an important factor having a substantial role when considering the properties of a material, including tribo-electrification. The samples were analysed and differences in the x-ray diffraction patterns between 5° and 100° at angle $2\theta$ between the parent drug and their binary mixtures were compared. As shown in Figure 3, it is evident that mesoporous silica (SBA-15) is an amorphous material. There are some variances in the peak angle between the binary mixtures of FBP and SBA-15 prepared by solvent impregnation; in comparison to pure FBP drug which possesses characteristic peaks at, 7°, 11°, 16°, and 21°. The XRD pattern of binary mixtures prepared by physical impregnation demonstrates a slight decrease in peak size, in contrast with the pure drug. The most substantial difference being observed in 20% SBA-F.

## 3.3- Content uniformity analysis

Content uniformity of all the powder mixtures were quantified using UV-VIS spectroscopy. The percentage of drug loading was determined by dissolving the SBA-15: FBP powder mixture. The dissolved FBP was quantified by adopting the linear regression equation of the standard calibration curve of FBP. The linearity coefficient ($R^2$) was 0.994 and the findings showed all the binary powder mixtures contained 95-105% of FBP theoretical content, hence satisfying the criteria of British Pharmacopeia (BP 2012).

## 3.4- Pore size distribution and specific surface area measurement

The surface area and pore size distribution of SBA-15 and subsequent binary mixtures were determined by nitrogen adsorption at 77K and resulted are summarised in Table 2. The specific surface area of pure SBA-15 sample was found to be 744.6 $m^2/g^{-1}$ and significantly decreased to 6.4 $m^2/g^{-1}$ and 11.9 $m^2/g^{-1}$ in the case of the binary mixtures with FBP and SBA-15 prepared by solvent impregnation and physical impregnation respectively, at 5% SBA-15: FBP concentration. The data for 10% SBA-15 concentration showed a slight increase for both physical impregnation and solvent impregnation at 30.2 $m^2/g^{-1}$ and 13.7 $m^2/g^{-1}$ respectively in comparison to 5%. Results obtained for 15% SBA-15 display a specific surface area of 45.6 $m^2/g^{-1}$ for physical impregnation and 25.9 $m^2/g^{-1}$ for solvent impregnation. In comparison to 20% mesoporous silica which showed 58.2 $m^2/g^{-1}$ and 23.4 $m^2/g^{-1}$ for physical impregnation and solvent impregnation respectively. This data represents successful loading of FBP within the pores of the SBA-15, however, the degree of drug loading within the SBA-15 pore network was greater for the solvent impregnation technique in comparison to the physical impregnation method. Confirmation of successful drug loading is imperative as it indicated that drug loading technique does play a role, in the degree of drug uptake as well as tribo-charging of the material. The greater the drug loading within the pores results in a reduced amount of drug material available to charge. The pore volume data was obtained using Barrett-Joyner-Halenda (BJH)

analysis. The method utilises a modified kelvin equation which accounts for the quantity of adsorbate removed from the pores as there is a decrease in relative pressure from high to low. This in turn relates to the volume of pore data obtained. The mesoporous silica (SBA-15) had a mesoporous volume of 0.79 $cm^3$ $g^{-1}$ whilst the pore volume of binary mixtures was found to be 0.1 $cm^3$ $g^{-1}$ and below depending on the SBA -15 concentration, as well as the loading technique utilised indicating the successful inclusion of FBP within the highly porous silica. The solvent impregnation technique results in binary mixtures with a smaller surface area as well as pore volume when compared to the physical impregnation method.

## 3.5- Tribo-electrification and powder surface adhesion studies

The charge of the samples was measured at time intervals of 0.5, 2, 5 and 10 minutes with an initial charge recorded at time point zero which represents the charge on the sample prior being subjected to tribo-electrification. The data presented represent an average of three independent measurements obtained. The adhesion value refers to the mass loss of powder which strongly adhered to the shaking container (Figures S1-S2). The electrostatic charge level of the model drug increased with shaking time where a maximum electronegative charge of -226 nC $g^{-1}$ (Figure 4) reached after 5 minutes of shaking. This indicates the movement of electrons from walls of the shaker to the drug particles which might be due to the higher work function of the FBP, resulting in a gain of electrons.

The triboelectric charge of SBA-15 was also measured and obtained at the time intervals mentioned above. SBA-15 has an extremely low charging tendency as a small charge to mass ratio was produced. The sample charged negatively against the stainless steel shaker at each time interval, with a reduction in charge level with shaking time towards electropositive until a charge level of -1.2 nC $g^{-1}$ was reached after 10 mins (Figure 4).

The SBA-15 produced a negative charge due to the transfer of electrons from the wall of the shaker to the powder particles as a result of the walls of the capsule possessing a lower work function. When comparing the adhesion data of the SBA-15 (Figure S1) to the model drug (Figure S2) it is evident that there is a vast reduction in tendency of the powder to adhere to the walls, FBP shows approximately 45% adhesion when induced to the shaking motion for 5 minutes in comparison to SBA-15 which had a maximum adhesion of approximately 18% after 10 minutes. The adhesion of the material to the shaker walls occurs due to the formation of an electric field, affecting the potential difference and resulting in greater adhesion. All mixtures were subjected to tribo-charging for 5 minutes, the charge results of the binary mixture produced by solvent impregnation method show that the highest charging sample was 5% SBA-F (Figure 5), the charging ranged from approximately -2.0 to -10 nC/g in comparison to FBP (-226 nC/g), Figure 4. It is evident from the data produced that the charging and adhesion is vastly affected by the ratio of the two samples in the mix. As the ratio of SBA-15 increased from 5% to 20% the charge level reduced, also from the adhesion data (Figure 6) it is apparent that the sticking propensity has reduced to below 14% for all ratios chosen for solvent impregnation in comparison to FBP at approximately 45%. There is an obvious reduction when as little as 5% of SBA is used. This reduction in charge and adhesion could be due to the change in particle-particle interactions between the FBP particles, due to the drug incorporating within the pores of the SBA-15, which acts as a low-charging carrier system, as drug only results in FBP particles induced to lateral motion upon other drug particles. As the concentration of SBA-15 has increased the probability of drug entering the pores increases, reducing the quantity of the highly charging and sticking drug available to be induced to tribo-electrification with the shaking container walls, the remainder drug material is induced to drug-SBA-15 interactions reducing the probability of drug-drug interactions. All samples charged negatively against the stainless steel container due to having a higher work function than the capsule and accepting

the charge transfer in accordance to the electron transfer theory. The charge and percentage adhesion data obtained for the physical impregnation sample was also investigated at a time interval of 5 minutes. From Figure 5 it is apparent that the charge of the powder mix decreased however not as significantly as when preparing by solvent impregnation. This may be due to a reduced chance of FBP loading within the pores as any agglomerates would be too large to enter the pores, which is evident from the BET data showing a larger surface area available after drug loading had occurred in comparison to the solvent impregnation method. The charging decreased as the percentage of SBA-15 increased form 5% to 20%. Like the solvent impregnation method, the physical impregnation did reduce the percentage adhesion (Figure 6) of particles to the capsule walls and charging propensity of material, this was apparent when as little as 5% SBA-15 was used, resulting in better material handling properties.

## 4- Conclusions

The study confirms that the drug loading method and quantity of SBA-15 as the non-charging carrier system proposed in this work have an effect on the tribo-charging propensity and adhesion behaviour of FBP. It is commonly known that FBP has a tendency to charge significantly, hence used as a model drug within this study. FBP produced a saturated charge level of -226.4 nC/g and surface adhesion of 45%. With potential complications arising during powder handling, such as flowability of the material and poorer content uniformity. Changes to the particle to particle as well as particle to wall interactions have shown to modify the electrostatic properties of FBP due to its inclusion within the non-charging carrier SBA-15 system, which was demonstrated by the results as the SBA-15 concentration increased, the charging tendency and adhesion tendency of the material reduced drastically in comparison to FBP on its own. The drug loading method utilised did not vastly affect the results, as both

loading techniques reduced the net charge and percentage adhesion significantly in comparison to the parent drug. The solvent impregnation method saw a greater reduction in charge when compared to physical impregnation, this is potentially due to a greater quantity of FBP entering the pores in comparison to physical impregnation whereby any agglomerates are too large to enter, would stick to the surface of the SBA-15 particles and play a role in increasing the probability of drug to drug interactions

## Acknowledgements

The authors would like to thank Professor Barbara Conway for proof reading the article and university of Huddersfield for financial assistance.

## References

Asare-Addo, K., Kaialy, W., Levina, M., Rajabi-Siahboomi, A., Ghori, M.U., Supuk, E., Laity, P.R., Conway, B.R., Nokhodchi, A., 2013. The influence of agitation sequence and ionic strength on in vitro drug release from hypromellose (E4M and K4M) ER matrices—The use of the USP III apparatus. Colloids and Surfaces B: Biointerfaces 104, 54-60.

Barrett, E.P., Joyner, L.G., Halenda, P.P., 1951. The determination of pore volume and area distributions in porous substances. I. Computations from nitrogen isotherms. Journal of the American Chemical Society 73, 373-380.

British Pharmacopoeia (2012) British Pharmacopoeia Commission; Stationery Office: London, UK.

Brunauer, S., Emmett, P.H., Teller, E., 1938. Adsorption of gases in multimolecular layers. Journal of the American Chemical Society 60, 309-319.

Carter, P.A., Cassidy, O.E., Rowley, G., Merrifield, D.R., 1998. Triboelectrification of Fractionated Crystalline and Spray-dried Lactose. Pharmacy and Pharmacology Communications 4, 111-115.

Colilla, M., Baeza, A., Vallet-Regí, M., 2015. Mesoporous Silica Nanoparticles for Drug Delivery and Controlled Release Applications, The Sol-Gel Handbook. Wiley-VCH Verlag GmbH & Co. KGaA, pp. 1309-1344.

Cross, J., 1987. Electrostatics: Principles, Problems and Applications. Adam Hilger, Bristol, UK.

Ghori, M. U., Ginting, G., Smith, A. M., Conway, B. R. (2014a). Simultaneous quantification of drug release and erosion from hypromellose hydrophilic matrices. International Journal of Pharmaceutics, 465(1-2), 405-412.

Ghori, M. U. (2014). Release kinetics, compaction and electrostatic properties of hydrophilic matrices (Doctoral dissertation) University of Huddersfield, Huddersfield, UK.

Ghori, M.U., Šupuk, E., & Conway, B. R. (2014b). Tribo-electric charging and adhesion of cellulose ethers and their mixtures with flurbiprofen. European Journal of Pharmaceutical Sciences, 65, 1-8.

Ghori, M.U., Šupuk, E., Conway, B.R., 2015. Tribo-electrification and Powder Adhesion Studies in the Development of Polymeric Hydrophilic Drug Matrices. Materials 8, 1482-1498.

Kaialy, W. (2016). A review of factors affecting electrostatic charging of pharmaceuticals and adhesive mixtures for inhalation. International Journal of Pharmaceutics, 503(1-2), 262-276.

Kwok, P.C.L., Chan, H.-K., 2008. Solid forms and electrostatic properties of salbutamol sulfate. In: DalbyRN et al., eds. Respiratory Drug Delivery. River Grove: Davis Healthcare International.

Lakhani, D., Deshpande, A., 2013. Engineering Solution for pharmaceutical processing – Powder Handling. World Journal of Pharmacy and Pharmaceutical Sciences 2, 4582-4591.

Matsusaka, S., Maruyama, H., Matsuyama, T., Ghadiri, M., 2010. Triboelectric charging of powders: A review. Chemical Engineering Science 65, 5781-5807.

Matsusaka, S., Masuda, H., 2003. Electrostatics of particles. Advanced Powder Technology 14, 143-166.

Murtomaa, M., Harjunen, P., Mellin, V., Lehto, V.-P., Laine, E., 2002. Effect of amorphicity on the triboelectrification of lactose powder. Journal of Electrostatics 56, 103-110.

Paul, S., Taylor, L.J., Murphy, B., Krzyzaniak, J.F., Dawson, N., Mullarney, M.P., Meenan, P., Sun, C.C., 2017. Powder properties and compaction parameters that influence punch sticking propensity of pharmaceuticals. International Journal of Pharmaceutics 521, 374-383.

Rudrangi, S. R. S., Kaialy, W., Ghori, M. U., Trivedi, V., Snowden, M. J., & Alexander, B. D. (2016). Solid-state flurbiprofen and methyl-β-cyclodextrin inclusion complexes prepared using a single-step, organic solvent-free supercritical fluid process. European Journal of Pharmaceutics and Biopharmaceutics, 104, 164-170.

Song, S.W., Hidajat, K., Kawi, S., 2005. Functionalized SBA-15 Materials as Carriers for Controlled Drug Delivery: Influence of Surface Properties on Matrix−Drug Interactions. Langmuir 21, 9568-9575.

Šupuk, E., Ghori, M.U., Asare-Addo, K., Laity, P.R., Panchmatia, P.M., Conway, B.R., 2013. The influence of salt formation on electrostatic and compression properties of flurbiprofen salts. International Journal of Pharmaceutics 458, 118-127.

441 Šupuk, E., Hassanpour, A., Ahmadian, H., Ghadiri, M., Matsuyama, T., 2011. Tribo-
442 Electrification and Associated Segregation of Pharmaceutical Bulk Powders. KONA Powder
443 and Particle Journal 29, 208-223.

444 Šupuk, E., Seiler, C., Ghadiri, M., 2009. Analysis of a Simple Test Device for Tribo-Electric
445 Charging of Bulk Powders. Particle & Particle Systems Characterization 26, 7-16.

446 Verma, P., Prajapati, S.K., Yadav, R., Senyschyn, D., Shea, P.R., Trevaskis, N.L., 2016. Single
447 Intravenous Dose of Novel Flurbiprofen-Loaded Proniosome Formulations Provides
448 Prolonged Systemic Exposure and Anti-inflammatory Effect. Molecular Pharmaceutics 13,
449 3688-3699.

450 Watanabe, H., Ghadiri, M., Matsuyama, T., Ding, Y. L., Pitt, K. G., Maruyama, H., Masuda,
451 H. (2007). Triboelectrification of pharmaceutical powders by particle impact. International
452 Journal of Pharmaceutics, 334(1-2), 149-155.

453 Yu, H., Zhai, Q.-Z., 2009. Mesoporous SBA-15 molecular sieve as a carrier for controlled
454 release of nimodipine. Microporous and Mesoporous Materials 123, 298-305.

455 Zhang, J., Ebbens, S., Chen, X., Jin, Z., Luk, S., Madden, C., Patel, N., Roberts, C.J., 2006.
456 Determination of the Surface Free Energy of Crystalline and Amorphous Lactose by Atomic
457 Force Microscopy Adhesion Measurement. Pharmaceutical Research 23, 401-407.

458
459

460

461

462

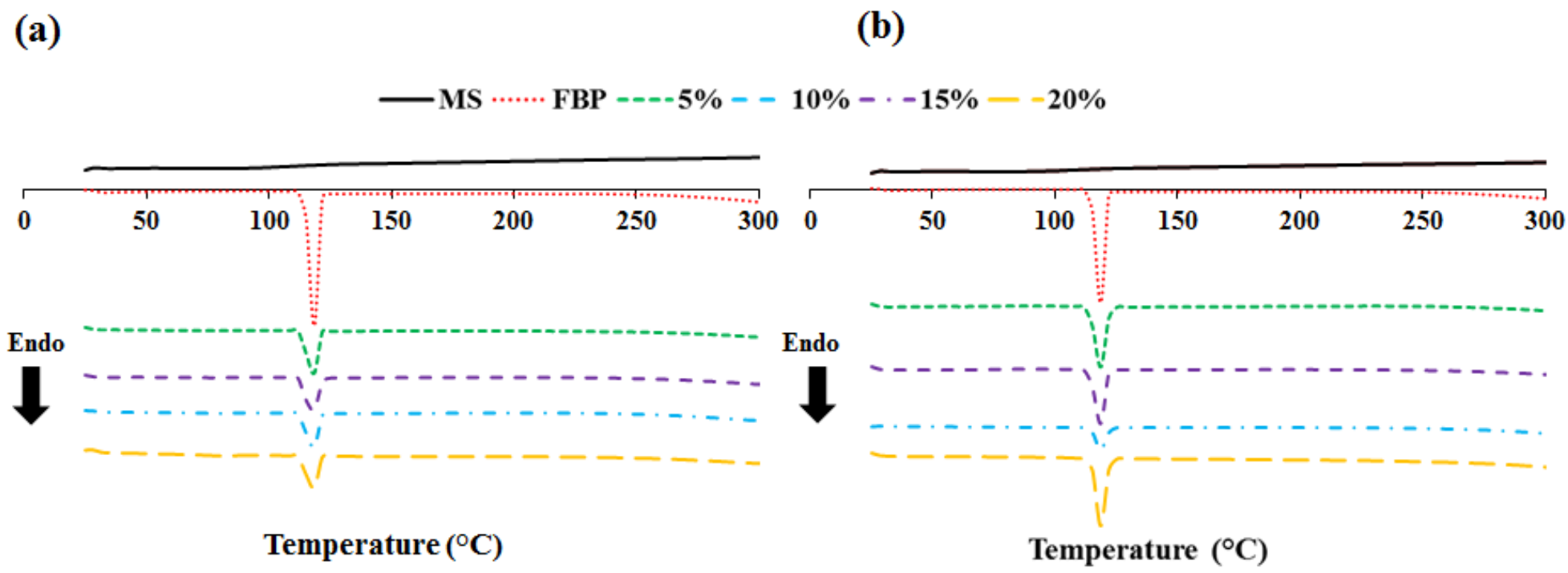


**Figure 1, DSC profiles of pure SBA-15, FBP and their respective powder mixture prepared by (a) physical mixing and (b) solvent impregnation.**

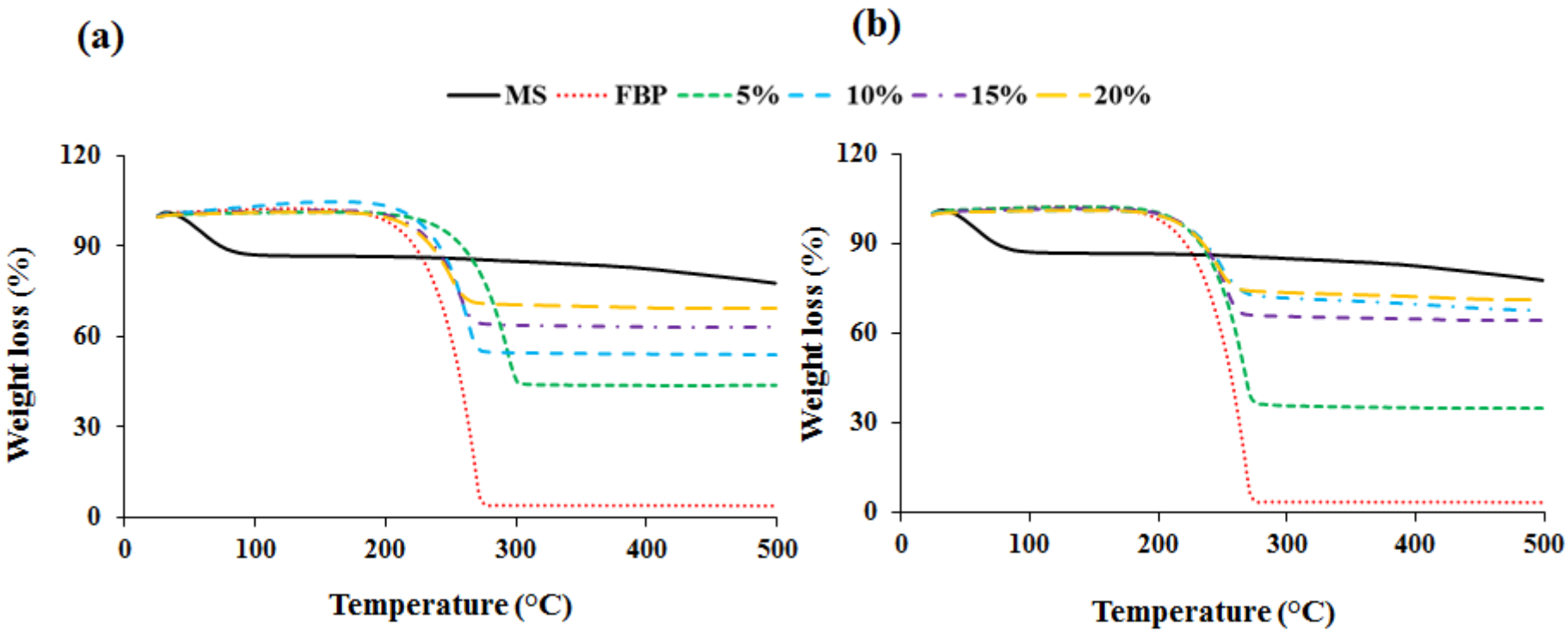


**Figure 2, TGA profiles of pure SBA-15, FBP and their respective powder mixture prepared by (a) physical mixing and (b) solvent impregnation.**

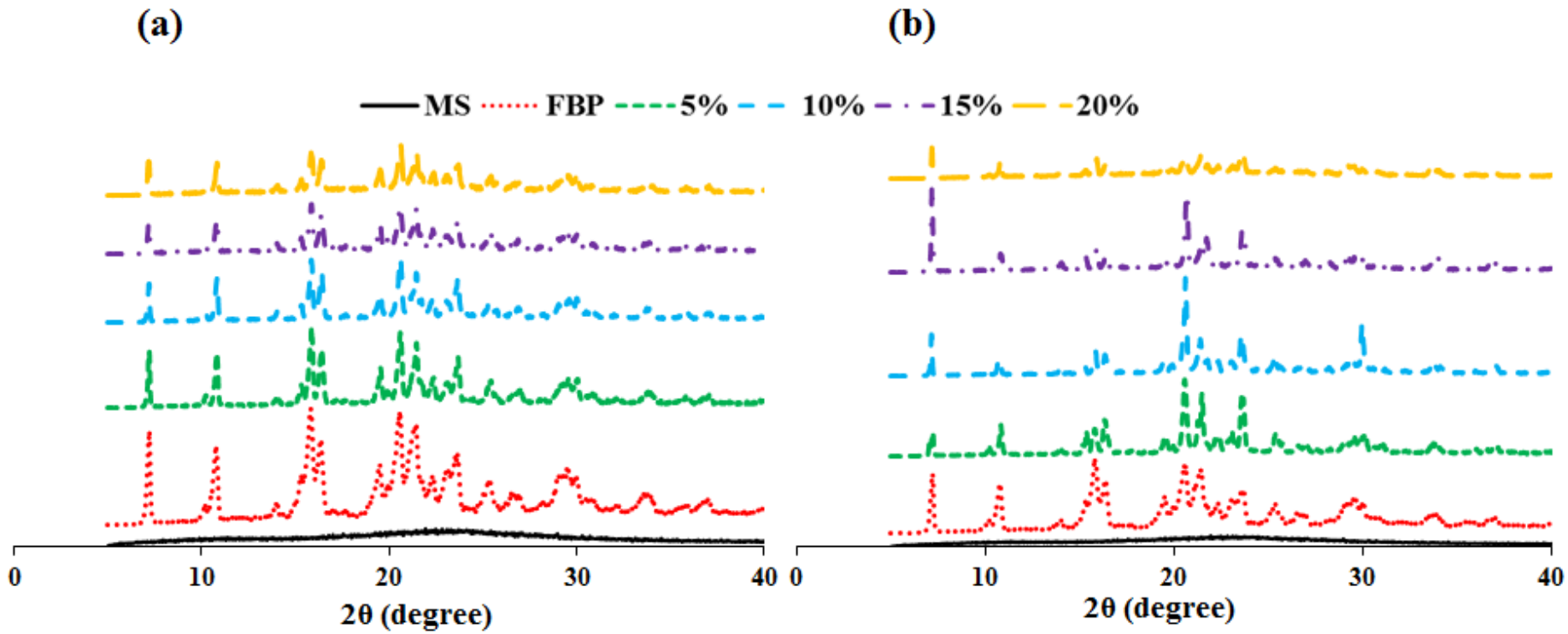


**Figure 3, XRD profiles of pure SBA-15, FBP and their respective powder mixture prepared by (a) physical mixing and (b) solvent impregnation.**

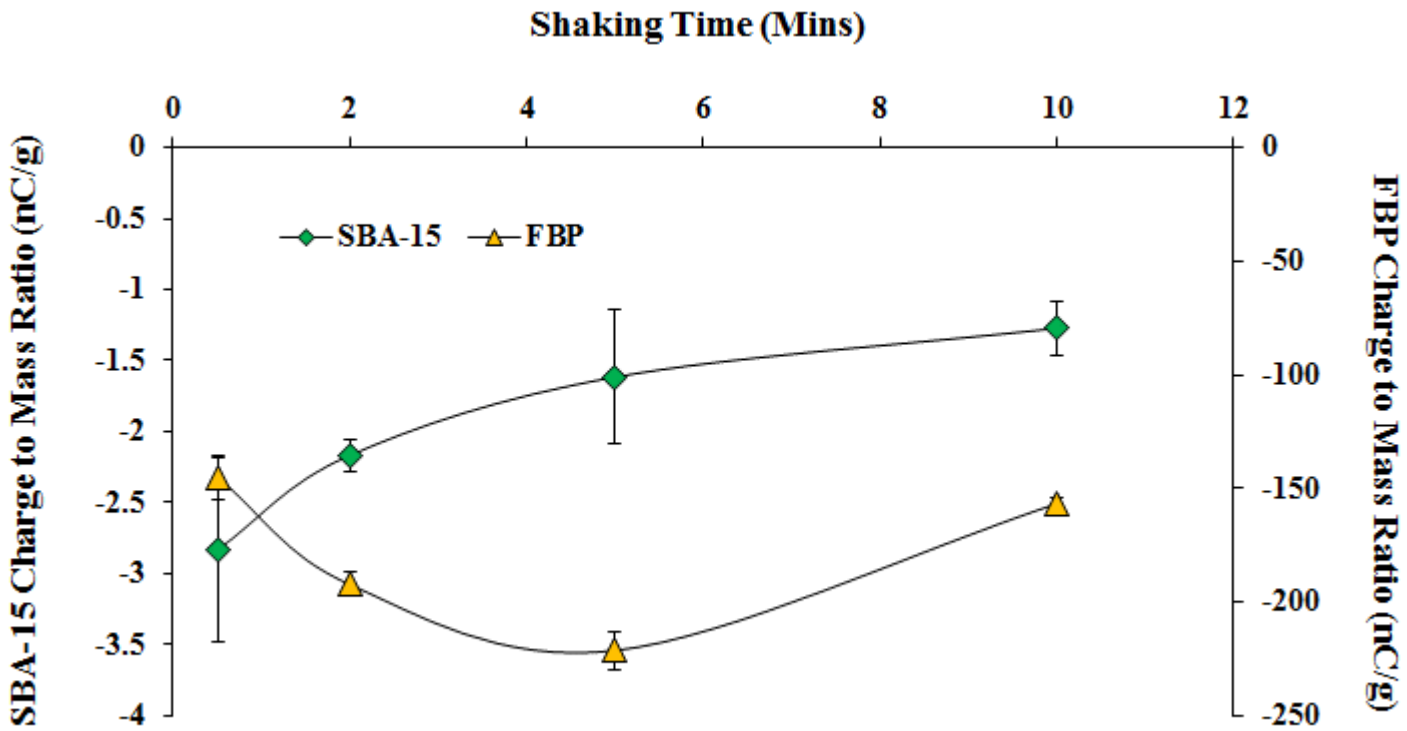


**Figure 4, Tribo-electric charging profiles of pure SBA-15 and FBP with respect to shaking time**

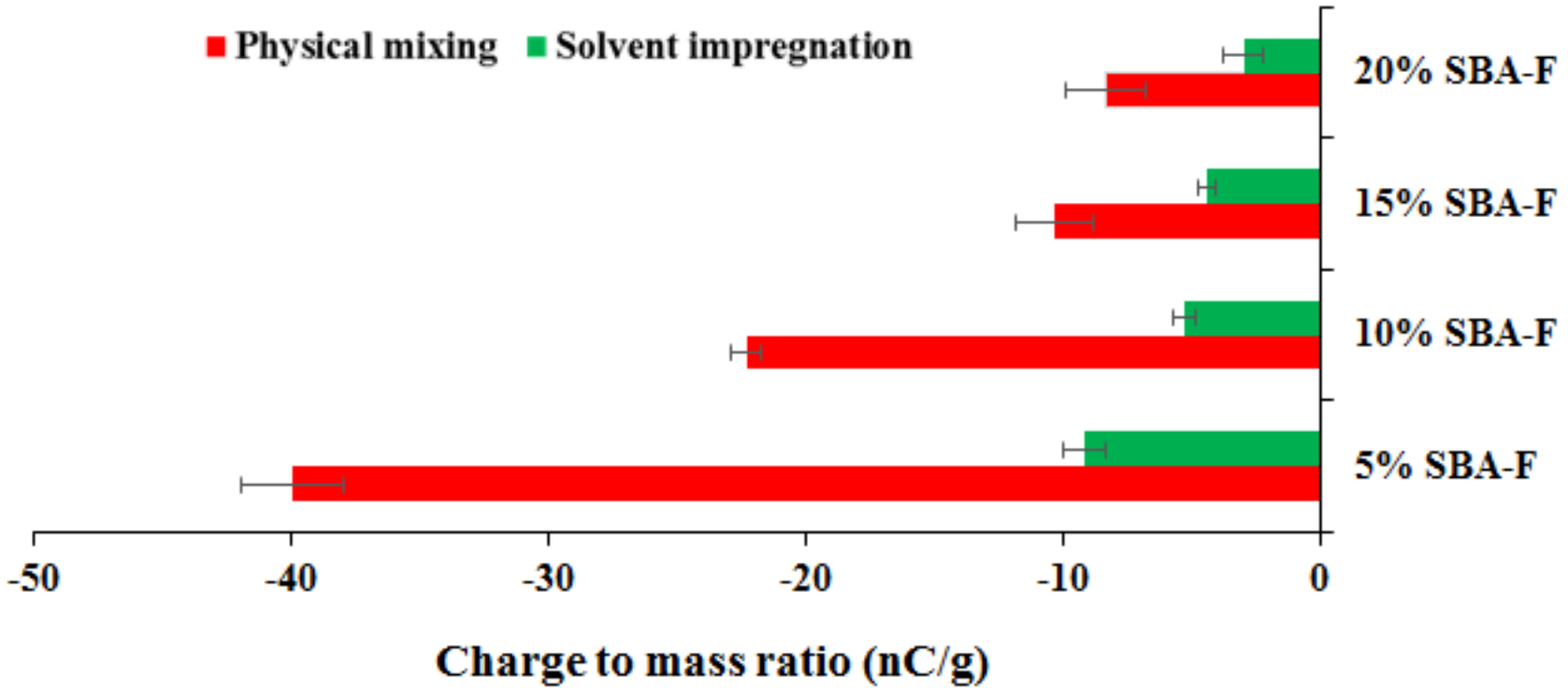


**Figure 5, Charge to mass ratio as a function of shaking time inside a stainless steel container at 20 Hz and a temperature of 22 °C with the relative humidity at 37.5% for SBA-FBP mixture produced by physical mixing and solvent impregnation.**

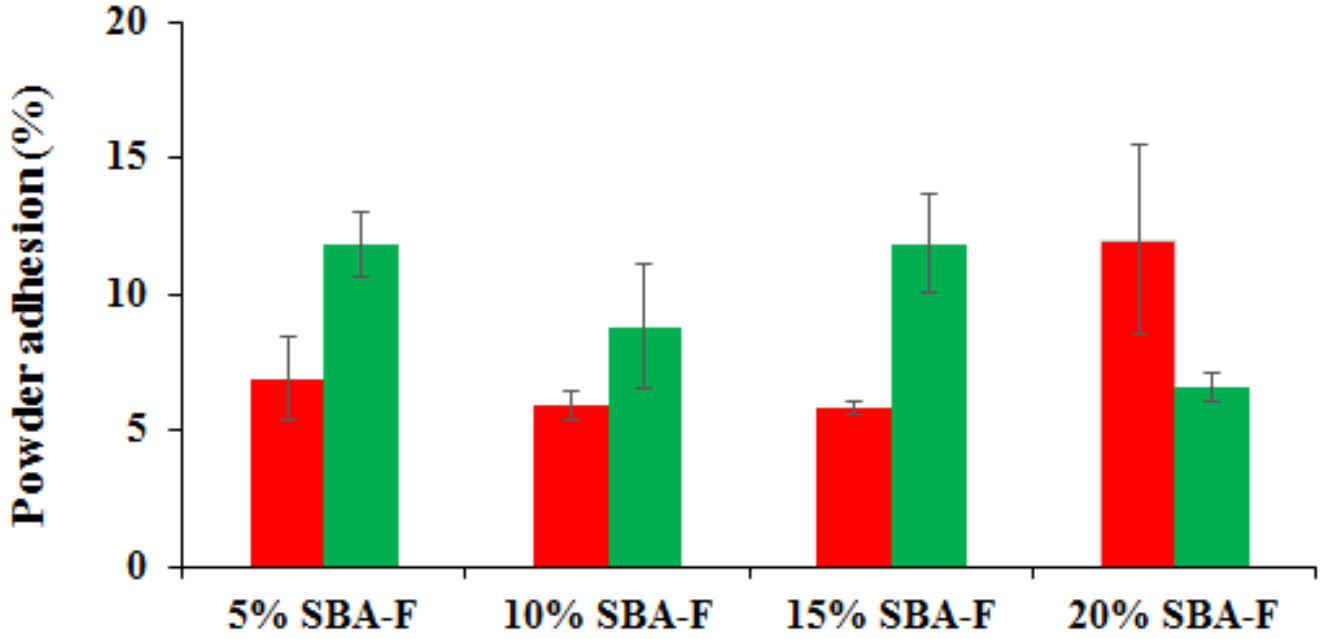


**Figure 6, The particle adhesion to stainless steel container walls after shaking at 20 Hz at 22.4°C and relative humidity 37.5% of the binary mixtures of FBP and SBA-15 that were prepared by physical mixing and solvent impregnation.**

**Table1, Summary of DSC melting parameters and relative crystallinity (%) of FBP and its powder mixtures**

| Sample | Melting peak (°C) | Melting enthalpy ($Jg^{-1}$) | Relative crystallinity (%) |
|---|---|---|---|
| **Flurbiprofen** | 116.6 | -116.5 | 100 |
| **5% SBA (PM)** | 116.67 | -107.9 | 92.61 |
| **10% SBA (PM)** | 116.44 | -102.22 | 87.74 |
| **15% SBA (PM)** | 116.79 | -84.74 | 72.73 |
| **20% SBA (PM)** | 116.42 | -71.48 | 61.35 |
| **5% SBA (SI)** | 119.21 | -101.58 | 87.19 |
| **10% SBA (SI)** | 117.15 | -89.75 | 77.03 |
| **15% SBA (SI)** | 117.54 | -67.86 | 58.24 |
| **20% SBA (SI)** | 118.16 | -61.23 | 52.55 |

SI = solvent impregnation, PM = Powder mixtures

**Table 2, Average pore diameter, specific surface area, and pore volume (pore sizes from17.000 Å to 3000.000 Å) for SBA-15 and the binary mixtures of FBP and SBA-15 prepared by solvent impregnation and physical mixing**.

| | **Pure Compounds** | | **Physical Mixing** | | | | **Solvent Impregnation** | | | |
|---|---|---|---|---|---|---|---|---|---|---|
| | SBA | FBP | 5% SBA-F | 10% SBA-F | 15% SBA-F | 20% SBA-F | 5% SBA-F | 10% SBA-F | 15% SBA-F | 20% SBA-F |
| BET Surface Area/ $m^2$ $g^{-1}$ | 744.6 | - | 11.9 | 30.3 | 45.6 | 58.2 | 6.4 | 13.7 | 25.9 | 23.4 |
| BJH Adsorption cumulative surface area of pores between 17.000 Å to 3000.000 Å / $m^2$ $g^{-1}$1 | 520.9 | - | 11.3 | 34.7 | 53.3 | 68.8 | 5.9 | 14.4 | 28.7 | 26.7 |
| BJH Desorption cumulative surface area of pore between 17.000 Å to 3000.000 Å / $m^2$ $g^{-1}$ | 595.5 | - | 14.5 | 40.1 | 3.1 | 77.5 | 7.2 | 16.8 | 33.5 | 30.4 |
| BJH Adsorption cumulative pore volume between 17.000 Å to 3000.000 Å / $cm^3$ g-1 | 0.79 | - | 0.02 | 0.05 | 0.08 | 0.10 | 0.02 | 0.03 | 0.05 | 0.05 |
| BJH Desorption cumulative pore volume between 17.000 Å to 3000.000 Å / cm3 g | 0.82 | - | 0.4 | 0.5 | 0.5 | 0.5 | 0.5 | 0.3 | 0.3 | 0.2 |
| Adsorption average pore width (4V/A by BET) / Å | 44.1 | - | 61.8 | 62.7 | 64.5 | 64.3 | 57.0 | 62.4 | 62.6 | 67.5 |
| BJH Adsorption average pore width (4V/A) / Å | 60.5 | - | 71.2 | 62.1 | 61.9 | 59.9 | 80.7 | 72.8 | 66.5 | 70.7 |
| BJH Desorption average pore width (4V/A) / Å | 55.1 | - | 55.5 | 53.6 | 53.9 | 53.3 | 65.7 | 62.1 | 59.1 | 62.0 |